AFRL-AFOSR-JP-TR-2019-0021

Bio-inspired GPS-free navigation using mantis shrimp (stomatopod) vision

Justin Marshall
THE UNIVERSITY OF QUEENSLAND
UNIVERSITY OF QUEENSLAND
BRISBANE, 4072
AU

03/20/2019
Final Report

Air Force Research Laboratory
Air Force Office of Scientific Research
Asian Office of Aerospace Research and Development
Unit 45002, APO AP 96338-5002

REPORT DOCUMENTATION PAGE

Form Approved
OMB No. 0704-0188

1. REPORT DATE *(DD-MM-YYYY)*	2. REPORT TYPE	3. DATES COVERED *(From - To)*
20-03-2019	Final	01 Sep 2017 to 31 Aug 2018

4. TITLE AND SUBTITLE
Bio-inspired GPS-free navigation using mantis shrimp (stomatopod) vision

5a. CONTRACT NUMBER

5b. GRANT NUMBER
FA2386-17-1-4077

5c. PROGRAM ELEMENT NUMBER
61102F

6. AUTHOR(S)
Justin Marshall

5d. PROJECT NUMBER

5e. TASK NUMBER

5f. WORK UNIT NUMBER

7. PERFORMING ORGANIZATION NAME(S) AND ADDRESS(ES)
THE UNIVERSITY OF QUEENSLAND
UNIVERSITY OF QUEENSLAND
BRISBANE, 4072 AU

8. PERFORMING ORGANIZATION REPORT NUMBER

9. SPONSORING/MONITORING AGENCY NAME(S) AND ADDRESS(ES)
AOARD
UNIT 45002
APO AP 96338-5002

10. SPONSOR/MONITOR'S ACRONYM(S)
AFRL/AFOSR IOA

11. SPONSOR/MONITOR'S REPORT NUMBER(S)
AFRL-AFOSR-JP-TR-2019-0021

12. DISTRIBUTION/AVAILABILITY STATEMENT
A DISTRIBUTION UNLIMITED: PB Public Release

13. SUPPLEMENTARY NOTES

14. ABSTRACT
The PI has successfully completed the research propoals. They assessed the instrument and method that they developed for shortcomings and determined that the sensor system and measurement protocol were the best target for improvement, in particular to make the system compatible with an underwater vehicle. The team developed a preliminary model of the noise in the underwater light fields polarization state due to wave action at various wind speeds so that we can design the instrument to measure the highest signal-to-noise ratio features. Finally the team prototyped and assessed three different panoramic imaging techniques for measuring the underwater light field without moving parts: all three techniques are viable but the fisheye lens and multi-camera solutions use less custom hardware than the conical mirror technique. There are peer reviewed papers in progress; a PhD gradutate thesis was directly supported by this research grant.

15. SUBJECT TERMS
biological navigation, entanglement, superposition, non-GPS navigation

16. SECURITY CLASSIFICATION OF:			17. LIMITATION OF ABSTRACT	18. NUMBER OF PAGES	19a. NAME OF RESPONSIBLE PERSON
a. REPORT	b. ABSTRACT	c. THIS PAGE			CHEN, JERMONT
Unclassified	Unclassified	Unclassified	SAR		19b. TELEPHONE NUMBER *(Include area code)* 315-227-7007

Final Report for AOARD Grant

FA2386-17-1-4077
Bio-Inspired GPS-Free Navigation Using Mantis Shrimp (Stomatopod) Vision

November 29th, 2018

PI – Justin Marshall

Sensory Neurobiology Group
Queensland Brain Institute
University of Queensland
St Lucia
Brisbane
Queensland 4072
AUSTRALIA
Ph +61 (0)7 3365 1397
Fx +61 (0)7 3365 4522
Cell +61 (0)423 024 162

Period of Performance: 1 September 2017 – 31 August, 2018

Introduction

The plan for this post-doctoral research in the Queensland Brain Institute (QBI) at the University of Queensland (UQ) was to continue and expand on the work of Samuel Powell's doctoral thesis [1], retaining collaborative links to the other laboratories. Powell's thesis examines and quantifies polarized light underwater using new technology he helped design and tested, partly in Australia. One of his findings is that it is possible to use the patterns in the polarization state of underwater light-fields for navigation tasks such as maintaining a particular heading, or even determining global location. As a Ph. D. student in Professor Viktor Gruev's lab at Washington University in St. Louis, he helped develop a high-resolution, real-time, visible-spectrum polarization camera based on the Mantis Shrimp (Stomatopod) eye [2]. His contributions were the optimization of a critical step in the fabrication process, a polarimetric calibration methodology [3], real-time signal processing routines for viewing live polarization video [4], and at the core of his doctoral thesis, an underwater housing for the polarization camera—developed in collaboration with the marine biology labs of Professors Justin Marshall and Tom Cronin at QBI/UQ and the University of Maryland, respectively. The marine biologists on our team have used the camera system to investigate visual systems and behaviors of polarization-sighted marine animals [5], Powell's research has focused on investigating how we can navigate using the highly structured nature of the patterns we observe in the polarization state of background light underwater. One thing we don't know is if marine animals do this also, opening up whole new areas of both biological and applied engineering that will learn from each other.

Underwater light is typically highly polarized due to the high level of scattering in the marine environment [6]. The polarization state as a whole is derived from many factors—hydrosol concentrations, suspended particulates, surface waves, and atmospheric conditions including cloud cover and sun position [7]–[10]. One thing we have observed is that when the sun is un-occluded, the polarization angle of the light field is primarily influenced by its position. Using a combination of machine learning techniques with a simple physics-based model of underwater scattering, Powell has shown that it is possible to infer the sun's position from a set of polarization angle measurements taken at multiple compass headings [11]. Knowing the sun's position and the current time enables the use of classical celestial navigation techniques for maintaining a course or determining global location. While other groups have focused on performing navigation tasks using the underwater view of the celestial polarization patterns, to our knowledge we are the first to focus on using the horizontal light field for a practical navigation solution.

The primary research goals under the support of this funding was 1) to refine the underwater polarization navigation techniques Powell developed as a graduate student, and 2) to explore how polarization-sighted animals might use polarization signals for navigation. To summarize our accomplishments under this funding:

a) We assessed the instrument and method that Powell developed for shortcomings and determined that the sensor system and measurement protocol were the best target for improvement, in particular to make the system compatible with an underwater vehicle.
b) We developed a preliminary model of the noise in the underwater light field's polarization state due to wave action at various wind speeds so that we can design our instrument to measure the highest signal-to-noise ratio features.
c) We prototyped and assessed three different panoramic imaging techniques for measuring the underwater light field without moving parts: all three techniques are viable but the fisheye lens and multi-camera solutions use less custom hardware than the conical mirror technique.

These outputs are detailed below under the original aims of the proposal.

Aim 1: Improving polarization-based underwater navigation.

Over the course of developing our underwater celestial navigation solution, we identified several areas for improvement. The system is composed of several modular stages from the polarization sensor and measurement protocol to the various processing algorithms: sensor calibration, feature extraction, and inference. While improvement in any of these stages could increase navigation accuracy, we decided to focus our effort on improving the measurement protocol and sensor system for a variety of reasons.

The existing measurement system, as described in [11], consists of an almost completely custom underwater polarization video camera system. The CCD polarimeter [12], was hand-assembled and mounted in a rebuilt underwater camcorder housing with a compact PC and power supply. Physically, the system was about 40 cm (1'4") long and weighed about 10 kg (22 lbs). The system consumed approximately 20W of power and produced about 1 GB of data per minute of recording (the CPU was not powerful enough to both compress the data and display live polarization video simultaneously). This limited the system to approximately 2 hours of runtime, which could be extended to about 6 hours by running in a time-lapse mode. The camera system is good for general underwater polarization videography, as it was designed, but is inappropriate for certain navigation experiments such as long-term recordings or mounting on an autonomous or remotely operated underwater vehicle (AUV or ROV). The physical improvements we focused on were reducing the system size, weight, and power requirements, and updating the CPU to the current state-of-the-art.

The measurement protocol for the underwater navigation project consisted of setting the camera on a tripod and rotating it about the zenith axis to capture the horizontal light field. The pose of the camera was measured using a high-precision compass (magnetometer and accelerometer) package. While stationary, the compass gives heading, roll, and pitch with RMS error less than 0.5°, but the package does not have an integrated gyroscope, so it is unable to compensate for rotational movement. Thus, we had to pause the camera rotation regularly to let the compass settle before moving again. This slowed the measurement protocol so that each acquisition required approximately 2 minutes to complete. To improve the measurement protocol our goals were to reduce the number of measurements, focusing on those with the highest signal to noise ratio, and to reduce the level of human interaction so that the device could be used more easily with an AUV or ROV.

Aim 1.1: Underwater light field noise analysis

The most effective measurement strategy for the underwater light field will focus on the highest signal-to-noise ratio features (whether they or polarization signals or otherwise). Variations in the in-water light field are caused by movement of the sun, changing weather conditions, changing water quality, and waves at the water surface. In this case, the changes caused by the movement of the sun are our signal and we treat the remainder as noise sources. We focused our effort on simulating the noise contribution of water waves as it is both an obvious noise source and the most tractable.

Several groups have published on the use of the celestial polarization pattern as it is seen from underwater as a navigation cue [13], [14]. It would also be possible to use a direct observation of the sun from underwater for solar navigation. The purpose of this analysis was to determine which features are worth measuring under the noise of water waves: the intensity of the sky (including the image of the sun), the polarization of the sky, the in-water intensity, or the in-water polarization.

The noise analysis was performed numerically. First, wave height maps were generated for 3 and 10 m/s wind speeds using the Fourier transform method [15]. Wave slope histograms were computed from these. The SCIATRAN software package was used to simulate the celestial polarization patterns at various sun elevations [16], and these sky images were then refracted through each wave slope with weighted statistics accumulated according to the slope histograms. The SCIATRAN simulations do not include the direct image of the sun, so this was independently refracted through the wave surfaces. For the in-water noise, the same statistics were computed but instead of refracting the whole sky, the direct sun ray was refracted through each wave slope and then scattered once, as per [11].

The simulation results are presented in Figs. 1-3. It is clear from this analysis that there is less noise in the intensity channel than polarization when looking up at the sky from underwater, and less noise in the polarization than intensity for the scattered in-water light field. Because the strongest intensity feature in the sky is the image of the sun and it was not included in the same statistics due to the limitations of SCIATRAN, it is not fair to compare the noise levels of the intensity of the sky to the in-water polarization. However, our intuition is that in shallower waters it would make sense to look directly up at the sky and sun and in deeper waters, where the image of the sky is destroyed by forward scattering the in-water polarization patterns become more salient. A more comprehensive simulation or real-world measurements would be required to test where such a cross-over would happen.

Aim 1.2: Assessing panoramic polarization imaging techniques.

Reducing the level of human interaction required for measurements and increasing the speed of measurements are both necessary to integrate the system with an AUV or ROV. To this end, we assessed 3 established techniques for panoramic imaging, modified for polarimetric imaging: 1) Using a fish-eye lens with a field-of-view greater than 180°, 2) using a catadioptric (lens & mirror) panoramic camera, and 3) using multiple cameras arranged in a ring.

As described in [11], we have previously captured polarization imagery using a standard 185° fisheye lens on the polarization camera. For the navigation application, we require the polarization information about the horizon, which we can capture with the 185° lens pointing straight up. This strategy works, but has shortcomings. The biggest issue is that the percent of pixels imaging unimportant regions is quite high—leading to inefficiency in both the material cost of the system and the information that must be processed. The unimportant regions can also include overly bright areas outside the exposure range of the horizon, causing problems for auto-exposure algorithms, or in the worst case, excessive bloom that corrupts the important part of the image (see Fig. 4). In our assessment, the fisheye lens approach is workable, but not ideal.

Our second approach for capturing an underwater polarization panorama was the use of a catadioptric (i.e. combined refractive and reflective optics) panoramic camera [17], [18]. For polarization imaging, we made use of a standard Canon PowerShot S120 point-and-shoot camera aimed down at a conical mirror on loan from Prof. Srinivasan, also at the Queensland Brain Institute. Polarization filter rings were constructed from high-quality waterproof polarizing film cut into strips at 0°, 60°, and 120°, then wrapped into a tube and stabilized with wooden rings at either end (see Fig. 5). Photos were taken with each ring placed around the mirror in turn. The first trial of this system in air is illustrated in Fig. 5, successfully showing the expected polarization patterns of the sky. Unfortunately, when taken underwater (Fig. 6) the mirror tarnished within minutes, corrupting any polarization signal.

This prototype system was indeed less bulky than the original system and the use of commodity camera hardware reduced the system cost and complexity. However, the mirror was an

unfortunate combination of heavy and fragile, inappropriate for field work. To deploy the catadioptric system we would need to design and fabricate a custom mirror with the correct field of view and mount it within a glass dome or tube housing to prevent tarnishing. The system did require human interaction to swap the polarization filters, but this could be avoided by constructing a tube from appropriately patterned polarization film. Our final assessment was again that the system is workable, but designing a custom mirror and housing for it was prohibitive.

The final panoramic system we assessed was based on recording from multiple small wide-angle fixed-focus cameras simultaneously. We constructed the system using an NVIDIA Jetson TX1 embedded computer with the Auvidea M100 and J106 add-on boards for connecting to 3 Sony IMX-219 cameras, a battery, and storage. The entire system fit within a Nikon DSLR underwater housing with a 6" dome port. The same polarization filter tube system as used with the catadioptric system was employed for polarization imaging. To prevent the image of the surface from reflecting off the inside of the tube, a black cap was added to the top of each tube. The cameras were fitted with Demarren Technology Corp 190° fisheye lenses to achieve overlapping fields of view. Photos of the system and example measurements are shown in Fig. 7.

This system was the most convenient and flexible, given the form factor and use of small commodity cameras. However, combining the 3 frames into a seamless panorama will require at least geometric calibration of the cameras and testing of stitching algorithms. The Jetson CPU and cameras are efficient—we were easily able to record and compress HD video from the 3 cameras simultaneously for at least 4 hours on a 1.3 Ah capacity battery. This is the most promising panoramic imaging technique so far. The remaining challenge will be integrating polarization filters with the system so that human interaction is unnecessary.

Aim 2: Do marine animals use polarization for navigation?

The second aim of this research was to determine how marine animals could use the polarization features of the underwater light-field for navigation tasks. As an initial investigation, we have simulated the "squid's eye view" of the scattered in-water light as shown in Fig. 8. This simulation is based on the squid's retinal pattern, consisting of only vertical and horizontal polarization sensitivities, and the neurologically based "polarization distance" metric [19], [20]. The resulting pattern includes high-contrast spots both towards and away from the sun, which could easily be used as a compass cue by the animal. Interestingly, this limited view of the light field also includes sufficient information to infer the elevation of the sun in the sky. The pattern would also lend itself well to simple algorithms like centroid-finding, which could be of great benefit to the technical development of our navigation system.

References

[1] S. B. Powell, "Underwater Celestial Navigation Using the Polarization of Light Fields," Ph.D., Washington University in St. Louis, United States -- Missouri, 2017.

[2] T. York *et al.*, "Bioinspired polarization imaging sensors: From circuits and optics to signal processing algorithms and biomedical applications," *Proceedings of the IEEE*, vol. 102, no. 10, pp. 1450–1469, 2014.

[3] S. B. Powell and V. Gruev, "Calibration methods for division-of-focal-plane polarimeters," *Optics Express*, vol. 21, no. 18, pp. 21039–21055, 2013.

[4] T. York, S. B. Powell, and V. Gruev, "A comparison of polarization processing across different platforms," 2011.

[5] S. Johnsen, Y. L. Gagnon, N. J. Marshall, T. W. Cronin, V. Gruev, and S. Powell, "Polarization vision seldom increases the sighting distance of silvery fish," *Current Biology*, vol. 26, no. 16, pp. R752–R754, 22 2016.

[6] G. W. Kattawar, "Polarization of Light in the Ocean," in *Ocean optics*, R. W. Spinrad, K. L. Carder, and M. J. Perry, Eds. New York: Oxford University Press, 1994, pp. 202–225.
[7] T. H. Waterman, "Polarization Patterns in Submarine Illumination," *Science (New York, N.Y.)*, vol. 120, no. 3127, p. 927, 1954.
[8] V. A. Timofeeva, "Optics of turbid waters (results of laboratory studies)," *Optical Aspects of Oceanography*, 1974.
[9] Y. You *et al.*, "Measurements and simulations of polarization states of underwater light in clear oceanic waters," *Applied Optics*, vol. 50, no. 24, p. 4873, 2011.
[10] G. W. Kattawar, G. N. Plass, and J. A. Guinn Jr, "Monte Carlo calculations of the polarization of radiation in the earth's atmosphere-ocean system," *Journal of Physical Oceanography*, vol. 3, no. 4, pp. 353–372, 1973.
[11] S. B. Powell, R. Garnett, J. Marshall, C. Rizk, and V. Gruev, "Bioinspired polarization vision enables underwater geolocalization," *Science Advances*, 2018.
[12] V. Gruev, R. Perkins, and T. York, "CCD polarization imaging sensor with aluminum nanowire optical filters," *Optics Express*, vol. 18, no. 18, pp. 19087–19094, 30 2010.
[13] A. Lerner, S. Sabbah, C. Erlick, and N. Shashar, "Navigation by light polarization in clear and turbid waters," *Philosophical Transactions of the Royal Society of London B: Biological Sciences*, vol. 366, no. 1565, pp. 671–679, 2011.
[14] D. C. Parkyn, J. D. Austin, and C. W. Hawryshyn, "Acquisition of polarized-light orientation in salmonids under laboratory conditions," *Animal Behaviour*, vol. 65, no. 5, pp. 893–904, 2003.
[15] C. D. Mobley, "Polarized reflectance and transmittance properties of windblown sea surfaces," *Appl. Opt., AO*, vol. 54, no. 15, pp. 4828–4849, May 2015.
[16] V. V. Rozanov, A. V. Rozanov, A. A. Kokhanovsky, and J. P. Burrows, "Radiative transfer through terrestrial atmosphere and ocean: Software package SCIATRAN," *Journal of Quantitative Spectroscopy and Radiative Transfer*, vol. 133, pp. 13–71, Jan. 2014.
[17] J. S. Chahl and M. V. Srinivasan, "Reflective surfaces for panoramic imaging," *Appl. Opt., AO*, vol. 36, no. 31, pp. 8275–8285, Nov. 1997.
[18] R. Benosman, *Panoramic vision: sensors, theory, and applications.* New York: Springer, 2012.
[19] Talbot Christopher M. and Marshall Justin N., "The retinal topography of three species of coleoid cephalopod: significance for perception of polarized light," *Philosophical Transactions of the Royal Society B: Biological Sciences*, vol. 366, no. 1565, pp. 724–733, Mar. 2011.
[20] How Martin J. and Marshall N. Justin, "Polarization distance: a framework for modelling object detection by polarization vision systems," *Proceedings of the Royal Society B: Biological Sciences*, vol. 281, no. 1776, p. 20131632, Feb. 2014.

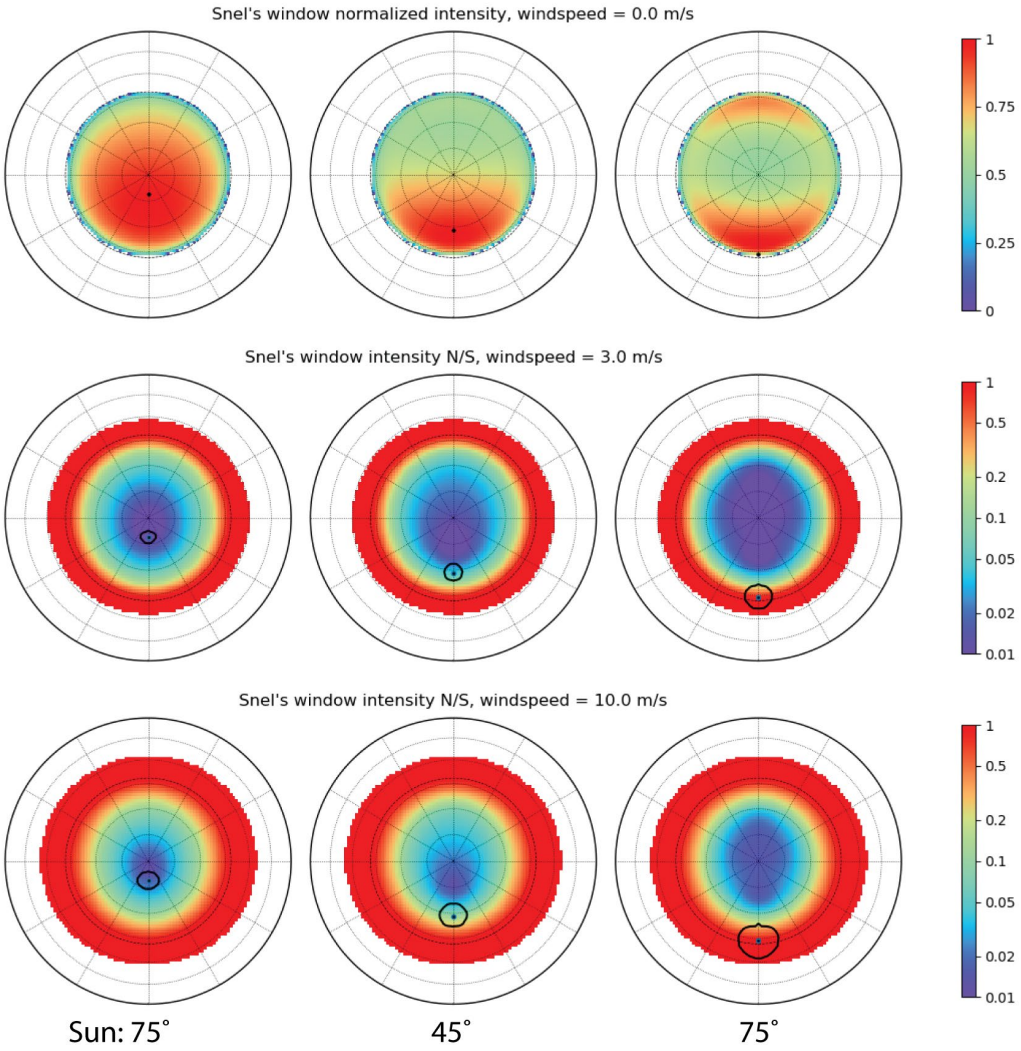

Figure 1. Simulated view of the sky through the water surface. Top row: normalized intensity, in false color. The sun's position is marked by a black dot. Middle and bottom rows: intensity noise due to waves at 3 m/s and 10 m/s wind speeds, respectively. The noise is normalized to the signal level to enable comparison. The contour around the sun's position surrounds the area that the sun's image is 99% likely to fall within. Each plot shows the entire hemisphere with the Lambert equal-area azimuthal projection—the centre is vertical and each concentric gridline is 15° down to the horizon. The extra dotted grid line is at 48°, the boundary of Snel's window with a flat surface.

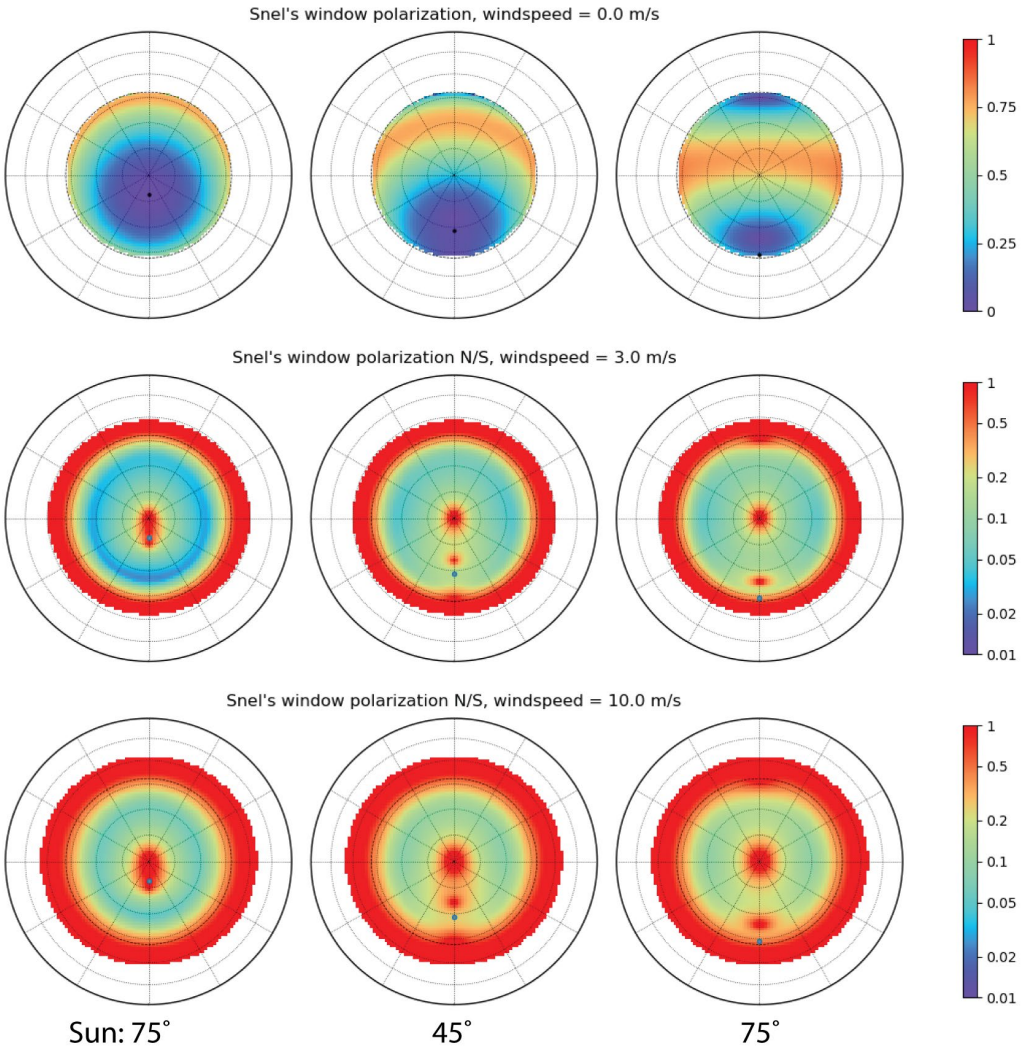

Figure 2. Simulated view of the sky through the water surface. Top row: degree of polarization. The sun's position is marked by a black dot. Middle and bottom rows: polarization noise due to waves at 3 m/s and 10 m/s wind speeds, respectively. The noise is normalized to the signal level to enable comparison. The polarization variance is measured by treating the (S1, S2) vector as Rayleigh distributed. Each plot shows the entire hemisphere with the Lambert equal-area azimuthal projection—the centre is vertical and each concentric gridline is 15° down to the horizon. The extra dotted grid line is at 48°, the boundary of Snel's window with a flat surface.

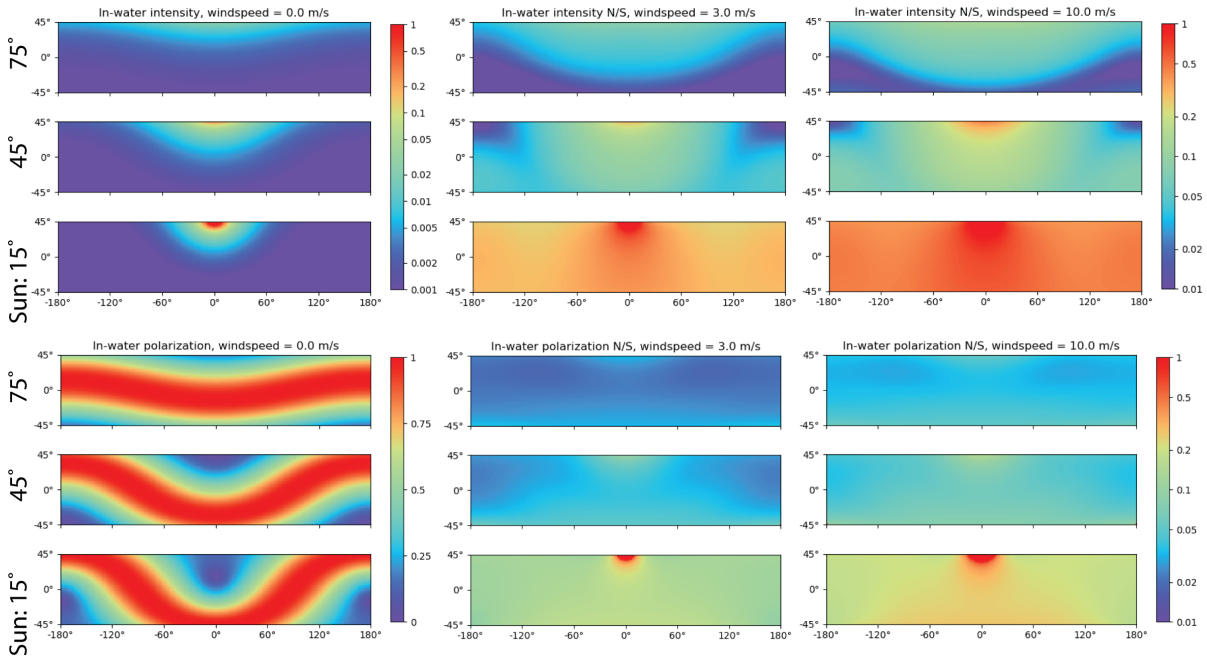

Figure 3. Scattered in-water light field. Left: patterns with a smooth water surface, middle: noise at 3 m/s wind, right: noise at 10 m/s wind. The noise levels are normalized to the signal so they can be compared. Top triplet: intensity, bottom triplet: polarization. The polarization variance is measured by treating the (S1, S2) vector as Rayleigh distributed.

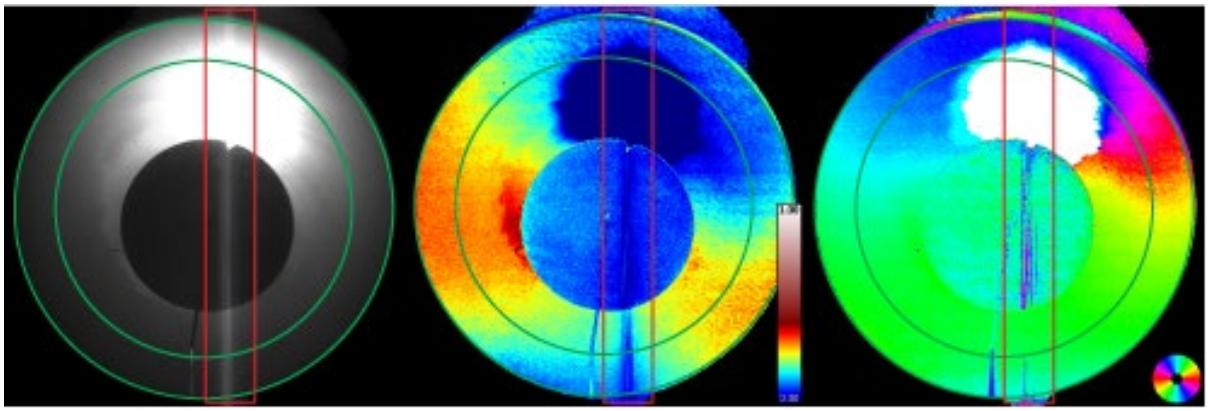

Figure 4. Polarization image captured with a 185° fish-eye lens. Left: intensity, middle: degree of polarization, right: angle of polarization. A metal disk is used to block direct sunlight from blooming on the image sensor. If the disk is not positioned accurately it both blocks a region we could have imaged and the bloom from the sun corrupts data across a large vertical region of the image (outlined in red). The region of interest for the navigation system is between the green rings.

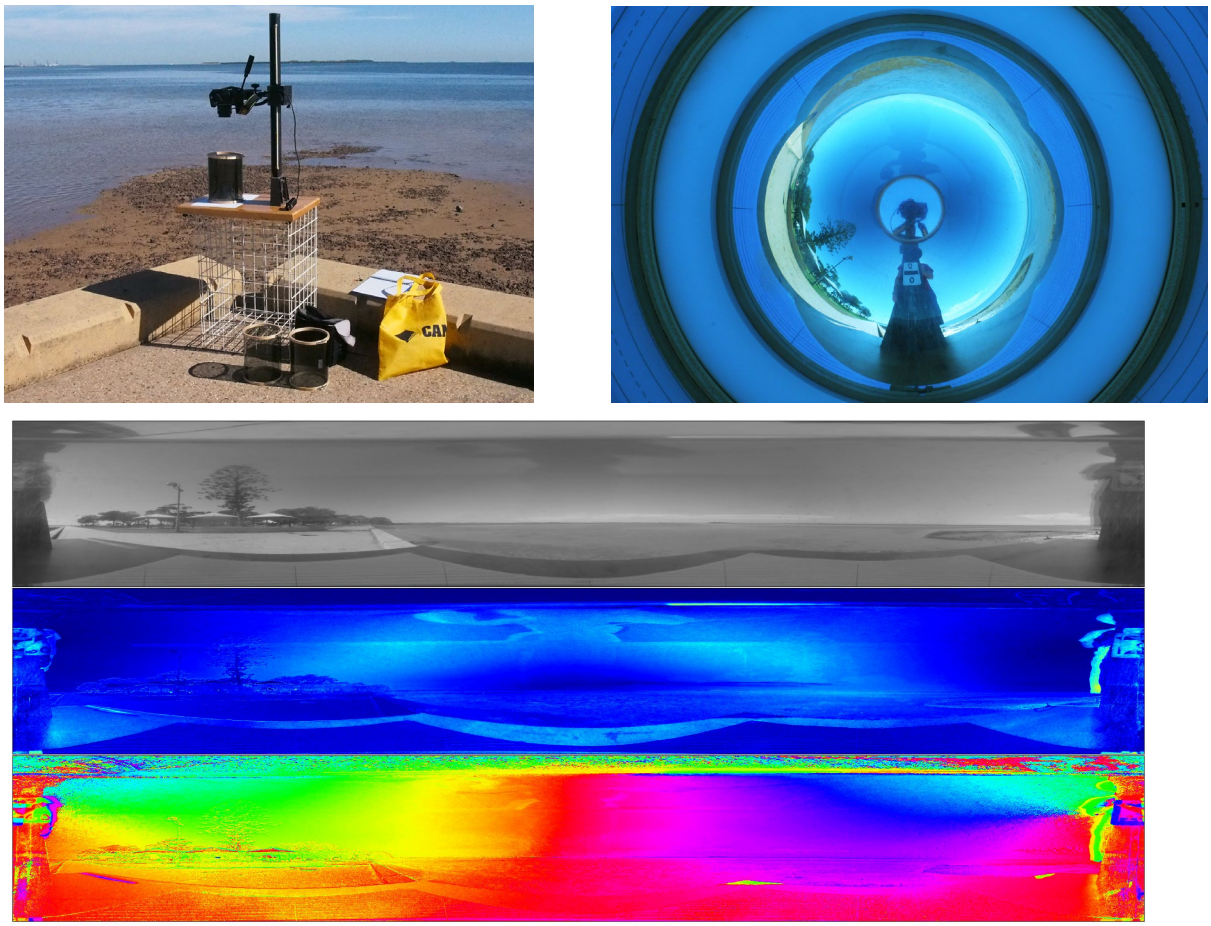

Figure 5. Catadioptric polarization imaging in air. Upper left: set-up with camera pointing down at a conical mirror with polarization filter tube, upper right: image captured by the set-up, lower strips: intensity image, degree of polarization, and polarization angle. In this case, the sun is blocked by the operator's body.

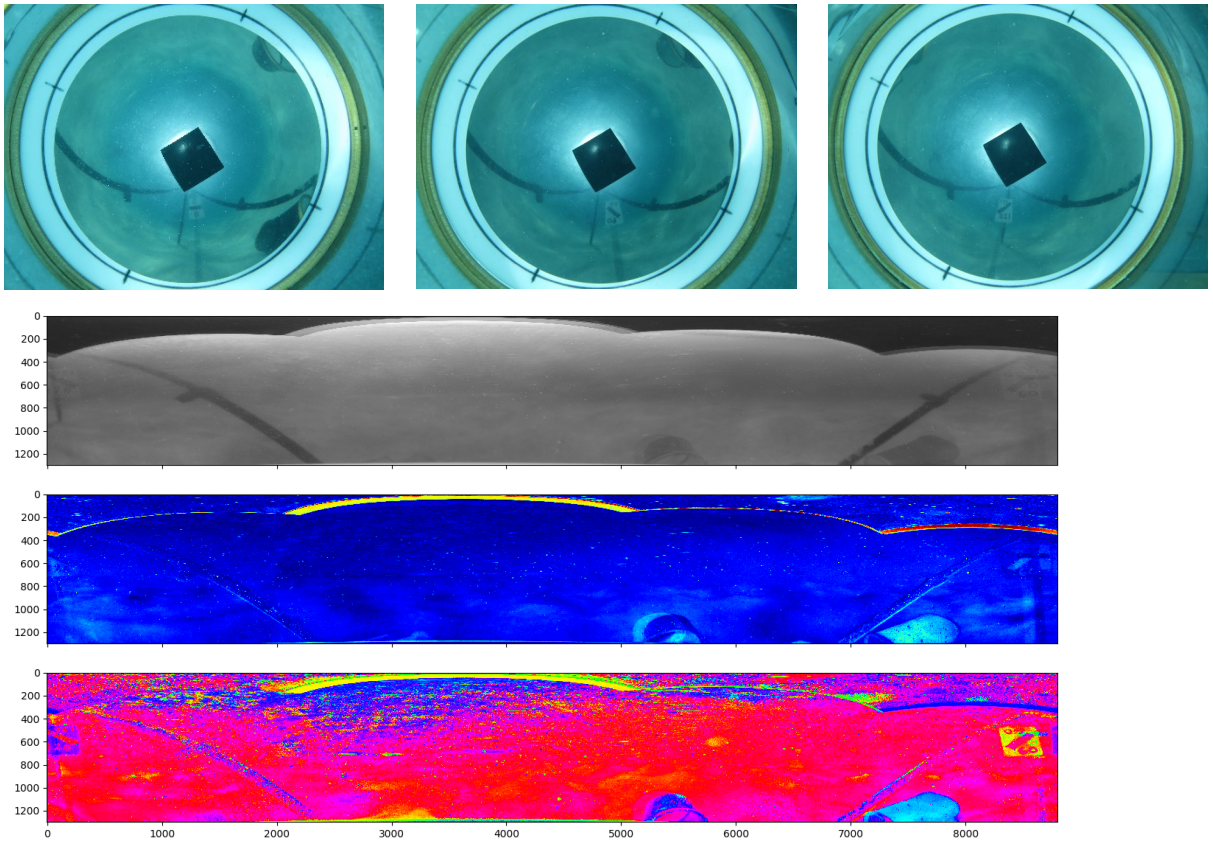

Figure 6. In the marine environment, the mirror tarnishes too quickly to obtain usable images, even when it's repolished before each dive. Top: images with each polarization filter (0°, 60°, 120°). A piece of vinyl tape blocks the reflection of the sun. Bottom: intensity, degree of polarization, and angle of polarization images—the noise from the tarnished mirror and slight shifts of the camera has destroyed any usable polarization signals.

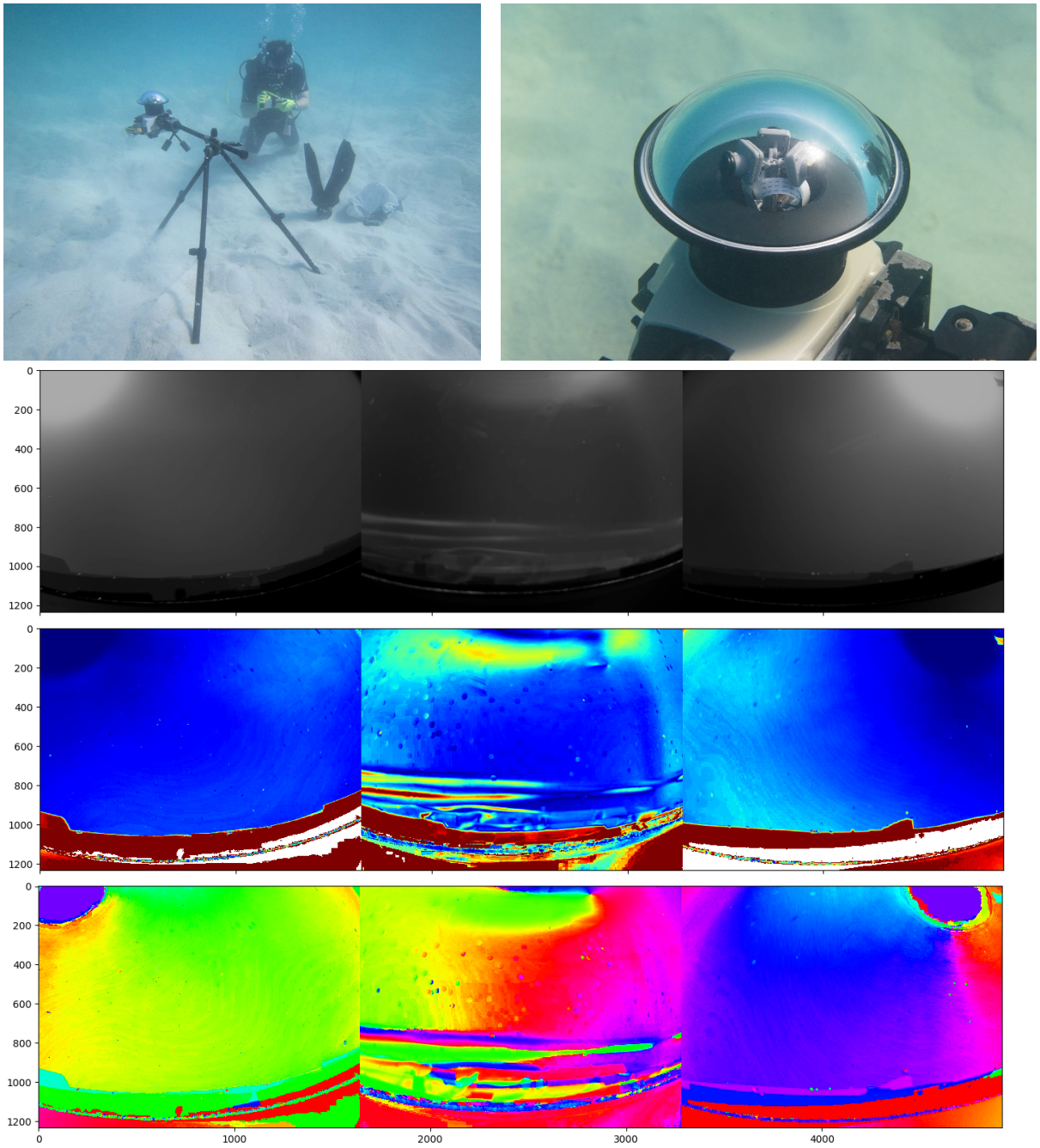

Figure 7. Multiple camera solution. Top: the camera system fits within a standard DSLR underwater housing. Bottom: intensity, degree of polarization and angle of polarization images. Bubbles and internal reflections from the polarizer tube (particularly visible in the center image) introduce confounding polarization signals, but the expected pattern is otherwise clearly visible.

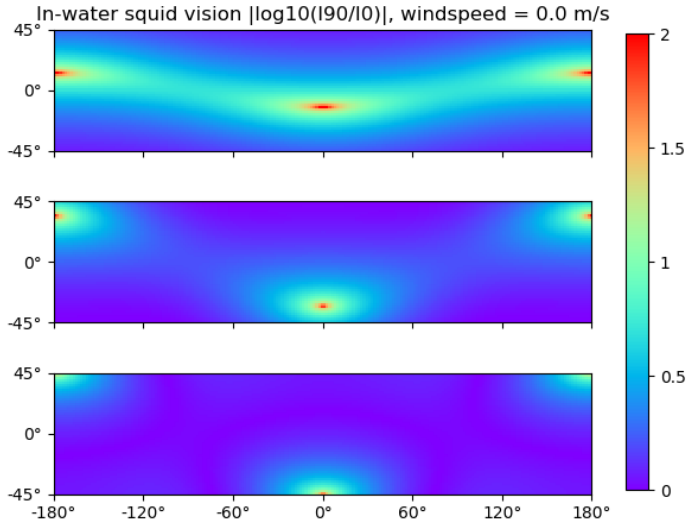

Figure 8. Squid's eye view of the scattered in-water light. Top to bottom: sun at 75°, 45°, and 15° elevation. The horizontal axis is the heading relative to the sun: the center is to the sun and the edges are away. Of note are the high-contrast spots at 0° and 180° heading, which would provide an easy navigation cue. Their elevation above and below the horizon is correlated to the elevation of the sun.